



Research article

Nonlinear higher-order time-fractional equations with purely integral boundary conditions: analytical results and numerical simulations

Ahcene Merad^{1,*} and Abdellah Menasri^{1,2}

¹ System Dynamics and Control Laboratory, Department of Mathematics and Informatics, Oum El Bouaghi University, Algeria

² Higher National School of Forests, Khenchela, Algeria

* **Correspondence:** Email: ahcene.merad@univ-oeb.dz.

Abstract: This paper studies a nonlinear higher-order time-fractional partial differential equation with purely integral boundary conditions in the strip $Q_T = (0, 1) \times (0, T)$. The model involves a Caputo derivative of order $0 < \alpha < 1$, a variable-coefficient principal part, and a nonlinear term depending on the solution and on its first spatial derivative. The analysis is formulated for any positive integer m under an explicit boundedness and coercivity hypothesis for the weak realization of the spatial operator on a moment-constrained space; this point is stated as a structural assumption, not as a consequence of positivity of the coefficient alone. We clarify the exact order of the variable-coefficient operator, construct a bounded lifting for the two imposed moments, give the weak duality formulation, and derive an a priori estimate with constants that do not depend on the unknown solution. Existence is obtained from a linear fractional solvability result and a fixed-point argument, while uniqueness and continuous dependence follow from a fractional energy inequality and a Mittag-Leffler version of the fractional Gronwall lemma. The numerical section is deliberately presented as a reproducible $m = 1$ validation: it includes the classical L1 finite-difference benchmark, a zero-moment forcing test, and an additional variable-coefficient nonlinear manufactured example solved by Picard iteration. The remaining extension to fully nonlinear higher-order discretizations for $m > 1$ is identified explicitly as future work.

Keywords: time-fractional partial differential equation; purely integral boundary conditions; Caputo derivative; weak solution; existence and uniqueness; continuous dependence; nonlocal constraints; L1 method

Mathematics Subject Classification: 35R11, 35K55, 65M06, 65M12

1. Introduction

Fractional evolution equations are widely used to model memory and hereditary effects that cannot be represented accurately by classical first-order time derivatives. In the present work we consider the nonlinear problem

$${}^c D_t^\alpha v(x, t) + (-1)^m \frac{\partial^{2m-1}}{\partial x^{2m-1}} \left(a(x, t) \frac{\partial v}{\partial x}(x, t) \right) = g \left(x, t, v(x, t), \frac{\partial v}{\partial x}(x, t) \right), \quad (x, t) \in (0, 1) \times (0, T), \quad (1.1)$$

subject to the initial condition

$$v(x, 0) = \phi(x), \quad x \in (0, 1), \quad (1.2)$$

and to two purely integral boundary conditions:

$$\int_0^1 \xi^i v(\xi, t) d\xi = e_i(t), \quad i \in \{0, 2m-1\}, \quad t \in (0, T). \quad (1.3)$$

Thus the notation in (1.3) means only the two indices $i = 0$ and $i = 2m - 1$; it does not mean the full set $\{0, 1, \dots, 2m - 1\}$. The compatibility relation at $t = 0$ is

$$\int_0^1 \xi^i \phi(\xi) d\xi = e_i(0), \quad i \in \{0, 2m-1\}. \quad (1.4)$$

The variable coefficient in (1.1) affects the structure of the spatial operator. If a is smooth, the Leibniz formula gives

$$\frac{\partial^{2m-1}}{\partial x^{2m-1}} (av_x) = a \partial_x^{2m} v + \sum_{\ell=0}^{2m-2} \binom{2m-1}{\ell} (\partial_x^{2m-1-\ell} a) \partial_x^{\ell+1} v. \quad (1.5)$$

Consequently, the strong expression has differential order $2m$ whenever a is sufficiently regular and bounded away from zero; the term $a \partial_x^{2m} v$ is the leading part, and derivatives of a produce lower-order terms. For nonconstant a , coercivity of the weak realization is therefore not a consequence of $a(x, t) > 0$ alone. In the analysis below, boundedness and coercivity of the complete weak form are stated explicitly as a structural hypothesis, and a sufficient route for verifying it in concrete coefficient classes is recorded in Theorem 2.5.

The mathematical difficulty comes from the simultaneous presence of a memory term, a higher-order spatial operator, variable coefficients, and nonlocal integral boundary constraints. Problems of fractional type and their analytic foundations can be found in the classical monographs of Podlubny and Kilbas–Srivastava–Trujillo [1, 2], and also in the works of Samko–Kilbas–Marichev and Diethelm [3, 4]. For time-fractional diffusion models and numerical approximation, standard references include Lin–Xu and Jin–Lazarov–Zhou [5, 6]. For nonlocal and integral boundary conditions, related perspectives appear in the literature on Bitsadze–Samarskii type problems [8], inverse and fractional diffusion-wave models [7], fractional equations with nonlocal boundary conditions [9], and Caputo–Hadamard integro-differential boundary conditions [10]. Recent work confirms that this area is still active. On the analytical side, well-posedness, regularity, and nonlocal boundary formulations for fractional evolution equations have been developed in several directions. These include diffusion problems with nonlocal or coupled conditions [11, 13, 20], fractional Langevin-type and sequential fractional systems [12, 15, 17],

Hilfer–Hadamard and delay-type systems with nonlocal conditions [16,21,22], and generalized nonlocal or integral boundary-value formulations [23,24,27]. Further recent examples are given by fractional evolution equations with multipoint or hybrid nonlocal conditions [28–30]. On the computational side, recent progress on L1-type and related high-order or structure-preserving schemes for time-fractional diffusion-type models can be found in [14,18,19] and in spectral or step-by-step approaches [25,26].

The contributions of the paper are the following.

- (i) We formulate (1.1)–(1.4) in a weak space adapted to the two imposed moments and give an explicit lifting that preserves time regularity.
- (ii) We prove a priori estimates, existence, uniqueness, and continuous dependence under stated assumptions on the weak spatial realization and on the Lipschitz nonlinearity. The constants are written so that their dependence on the final time and on the fractional Gronwall factor is visible.
- (iii) We provide a reproducible numerical section for the case $m = 1$. Besides the linear manufactured benchmark, we include a variable-coefficient nonlinear manufactured test. These computations support the second-order nonlocal discretization for $m = 1$, while the extension to fully higher-order nonlinear solvers remains outside the present numerical scope.

Throughout the paper, the right-hand side is interpreted consistently as $g(x, t, v, v_x)$ so that the equation is closed in the unknown v .

2. Preliminaries and definitions

Let $Q_T = (0, 1) \times (0, T)$, let $0 < \alpha < 1$, and let $m \geq 1$ be fixed.

Definition 2.1 (Caputo derivative). Let X be a Hilbert space. If $w \in H^1(0, T; X)$, the Caputo derivative of order α is

$${}^C D_t^\alpha w(t) = \frac{1}{\Gamma(1-\alpha)} \int_0^t (t-\tau)^{-\alpha} w'(\tau) d\tau = I^{1-\alpha} w'(t). \quad (2.1)$$

The integral is understood as a Bochner integral. Since the kernel $(t-\tau)^{-\alpha}/\Gamma(1-\alpha)$ belongs to $L^1(0, T)$ as a convolution kernel, Young's inequality gives

$$\|{}^C D_t^\alpha w\|_{L^2(0,T;X)} \leq \frac{T^{1-\alpha}}{\Gamma(2-\alpha)} \|w'\|_{L^2(0,T;X)}. \quad (2.2)$$

Thus the Caputo derivative is well defined in $L^2(0, T; X)$ when $w' \in L^2(0, T; X)$, even though the pointwise kernel is singular at $\tau = t$.

Definition 2.2 (Constraint space). The moment-constrained Sobolev space is

$$V_m^0 := \left\{ \psi \in H^m(0, 1) : \int_0^1 \psi(\xi) d\xi = 0, \int_0^1 \xi^{2m-1} \psi(\xi) d\xi = 0 \right\}. \quad (2.3)$$

Only these two moments are imposed because the original boundary data prescribe only the two quantities in (1.3). The intermediate moments $\int_0^1 \xi^k \psi(\xi) d\xi$, $1 \leq k \leq 2m-2$, are not constrained; adding them would define a different and overdetermined boundary-value problem.

Lemma 2.3 (Moment lifting). *There exist two polynomials $\eta_0, \eta_{2m-1} \in H^m(0, 1)$ such that*

$$\int_0^1 \eta_0(\xi) d\xi = 1, \quad \int_0^1 \xi^{2m-1} \eta_0(\xi) d\xi = 0, \quad \int_0^1 \eta_{2m-1}(\xi) d\xi = 0, \quad \int_0^1 \xi^{2m-1} \eta_{2m-1}(\xi) d\xi = 1. \quad (2.4)$$

Consequently, for $e_0, e_{2m-1} \in H^1(0, T)$, the function

$$z(x, t) = \eta_0(x)e_0(t) + \eta_{2m-1}(x)e_{2m-1}(t), \quad (2.5)$$

satisfies the two moment conditions and belongs to $H^1(0, T; H^m(0, 1))$. Moreover,

$$\|z\|_{H^1(0, T; H^m(0, 1))} \leq C_m (\|e_0\|_{H^1(0, T)} + \|e_{2m-1}\|_{H^1(0, T)}), \quad (2.6)$$

and

$$\|{}^C D_t^\alpha z\|_{L^2(0, T; H^m(0, 1))} \leq \frac{T^{1-\alpha}}{\Gamma(2-\alpha)} C_m (\|e_0\|_{H^1(0, T)} + \|e_{2m-1}\|_{H^1(0, T)}). \quad (2.7)$$

Proof. Take $p_0(x) = 1$ and $p_1(x) = x^{2m-1}$. The moment matrix

$$M = \begin{pmatrix} \int_0^1 p_0 dx & \int_0^1 p_1 dx \\ \int_0^1 x^{2m-1} p_0 dx & \int_0^1 x^{2m-1} p_1 dx \end{pmatrix} = \begin{pmatrix} 1 & (2m)^{-1} \\ (2m)^{-1} & (4m-1)^{-1} \end{pmatrix},$$

is nonsingular. Therefore, suitable linear combinations of p_0 and p_1 give η_0 and η_{2m-1} . The estimates follow immediately from the fixed polynomial norms and from (2.2). \square

Assumption 2.4 (Coercive realization of the principal operator). There is a bilinear form $B_t(\cdot, \cdot)$ on $V_m^0 \times V_m^0$, measurable in t , representing the weak realization of the spatial operator in (1.1). The same notation is used for its bounded extension to $H^m(0, 1) \times V_m^0$. We assume that there exist constants $c_A > 0$ and $C_A > 0$ such that

$$|B_t(u, \psi)| \leq C_A \|u\|_{H^m(0, 1)} \|\psi\|_{H^m(0, 1)}, \quad (2.8)$$

$$B_t(u, u) \geq c_A \|u\|_{H^m(0, 1)}^2, \quad (2.9)$$

for all $u, \psi \in V_m^0$ and almost every $t \in (0, T)$.

Remark 2.5 (How the coefficient derivatives enter). Assumption 2.4 is a structural hypothesis on the full weak form, not merely on the coefficient a . Formula (1.5) shows that the derivatives $\partial_x^r a$, $1 \leq r \leq 2m-1$, generate lower-order terms. A standard sufficient verification is the following: assume $a \in W^{2m-1, \infty}(Q_T)$, $a(x, t) \geq a_* > 0$, and suppose that, after the integrations by parts used to define B_t , one has

$$B_t(u, u) = \int_0^1 a(x, t) |\partial_x^m u(x)|^2 dx + \mathcal{L}_t(u, u), \quad |\mathcal{L}_t(u, u)| \leq \theta \|\partial_x^m u\|_{L^2(0, 1)}^2, \quad (2.10)$$

with $0 \leq \theta < a_*$. Since the two moment constraints imply a Poincaré-type estimate $\|u\|_{H^m} \leq C_{m, P} \|\partial_x^m u\|_{L^2}$ on V_m^0 , (2.9) follows with $c_A = (a_* - \theta)/C_{m, P}^2$. In concrete variable-coefficient problems, the number θ is obtained from bounds on the derivatives of a and from the boundary terms in the chosen weak realization.

Assumption 2.6 (Nonlinearity). The function $g = g(x, t, r, p)$ is measurable in (x, t) and globally Lipschitz in (r, p) : there exists $L_g > 0$ such that

$$|g(x, t, r_1, p_1) - g(x, t, r_2, p_2)| \leq L_g(|r_1 - r_2| + |p_1 - p_2|), \quad (2.11)$$

for all arguments. Moreover,

$$|g(x, t, r, p)| \leq c_0(x, t) + c_1|r| + c_2|p|, \quad (2.12)$$

where $c_0 \in L^2(Q_T)$ and $c_1, c_2 \geq 0$ are constants.

Assumption 2.7 (Data). The coefficient $a \in W^{2m-1, \infty}(Q_T)$ satisfies

$$0 < a_* \leq a(x, t) \leq a^* < \infty, \quad \text{for almost every } (x, t) \in Q_T, \quad (2.13)$$

and the data satisfy

$$\phi \in H^m(0, 1), \quad e_0, e_{2m-1} \in H^1(0, T), \quad (2.14)$$

together with the compatibility condition (1.4).

For a lifted function z from Lemma 2.3, write

$$v = w + z. \quad (2.15)$$

Then w satisfies the homogeneous moment constraints and belongs to V_m^0 in space.

Definition 2.8 (Weak solution). A function v is called a weak solution of (1.1)–(1.4) if $v = w + z$, where z is given by (2.5),

$$w \in L^2(0, T; V_m^0), \quad {}^C D_t^\alpha w \in L^2(0, T; (V_m^0)'), \quad (2.16)$$

$w(\cdot, 0) = \phi - z(\cdot, 0)$ in $L^2(0, 1)$, and

$$\langle {}^C D_t^\alpha w(t), \psi \rangle_{(V_m^0)', V_m^0} + B_t(w(t), \psi) = \langle G(t), \psi \rangle_{(V_m^0)', V_m^0}, \quad (2.17)$$

for every $\psi \in V_m^0$ and almost every $t \in (0, T)$, where

$$\langle G(t), \psi \rangle = \int_0^1 g(x, t, v(x, t), v_x(x, t)) \psi(x) dx - \langle {}^C D_t^\alpha z(t), \psi \rangle - B_t(z(t), \psi). \quad (2.18)$$

The duality pairing in (2.17) is the action of $(V_m^0)'$ on V_m^0 . When $w \in H^1(0, T; (V_m^0)'),$ it is explicitly

$$\langle {}^C D_t^\alpha w(t), \psi \rangle = \frac{1}{\Gamma(1-\alpha)} \int_0^t (t-\tau)^{-\alpha} \langle w'(\tau), \psi \rangle d\tau. \quad (2.19)$$

For general weak solutions, the same expression is understood in the distributional-in-time sense. The term ${}^C D_t^\alpha z$ in (2.18) is well defined in $L^2(0, T; H^m(0, 1)) \subset L^2(0, T; (V_m^0)'),$ by (2.7).

Remark 2.9 (Integrability of the nonlinear term). If $u, z \in L^2(0, T; H^m(0, 1))$ and $m \geq 1$, then $u + z$ and $(u + z)_x$ are in $L^2(Q_T)$. By (2.12), $g(x, t, u + z, (u + z)_x) \in L^2(Q_T)$. Therefore, it defines an element of $L^2(0, T; (V_m^0)'),$ through

$$\psi \mapsto \int_0^1 g(x, t, u + z, (u + z)_x) \psi(x) dx,$$

because $\|\psi\|_{L^2} \leq C \|\psi\|_{H^m}$ on V_m^0 .

Lemma 2.10 (Fractional Gronwall inequality). *Let $y \geq 0$ be locally integrable on $[0, T]$ and suppose that*

$$y(t) \leq a(t) + \frac{b}{\Gamma(\alpha)} \int_0^t (t-s)^{\alpha-1} y(s) ds, \quad 0 < t \leq T, \quad (2.20)$$

where a is nondecreasing and $b \geq 0$. Then,

$$y(t) \leq a(t)E_\alpha(bt^\alpha), \quad 0 \leq t \leq T, \quad (2.21)$$

where $E_\alpha(r) = \sum_{k=0}^{\infty} r^k / \Gamma(1 + k\alpha)$ is the one-parameter Mittag-Leffler function. If (2.20) is written without the factor $1/\Gamma(\alpha)$, then b in (2.21) is replaced by $b\Gamma(\alpha)$.

Lemma 2.11 (Caputo energy inequality). *Let H be a Hilbert space, and let $u \in H^1(0, T; H)$. For almost every $t \in (0, T)$,*

$$\langle {}^C D_t^\alpha u(t), u(t) \rangle_H \geq \frac{1}{2} {}^C D_t^\alpha \|u(t)\|_H^2. \quad (2.22)$$

Indeed,

$$\begin{aligned} 2 \langle {}^C D_t^\alpha u(t), u(t) \rangle_H - {}^C D_t^\alpha \|u(t)\|_H^2 &= \frac{t^{-\alpha}}{\Gamma(1-\alpha)} \|u(t) - u(0)\|_H^2 \\ &+ \frac{\alpha}{\Gamma(1-\alpha)} \int_0^t \frac{\|u(t) - u(s)\|_H^2}{(t-s)^{\alpha+1}} ds \geq 0. \end{aligned} \quad (2.23)$$

3. Main analytical results

Theorem 3.1 (A priori estimate). *Assume 2.4–2.7. Let $v = w + z$ be a weak solution of (1.1)–(1.4). Then,*

$$\begin{aligned} &\|w\|_{L^\infty(0,T;L^2(0,1))} + \|w\|_{L^2(0,T;H^m(0,1))} + \|{}^C D_t^\alpha w\|_{L^2(0,T;(V_m^0)')} \\ &\leq C_T (\|\phi - z(\cdot, 0)\|_{L^2(0,1)} + \|c_0\|_{L^2(Q_T)} + \|e_0\|_{H^1(0,T)} + \|e_{2m-1}\|_{H^1(0,T)}). \end{aligned} \quad (3.1)$$

The constant C_T depends on α , T , c_A , C_A , L_g , the embedding constants, and the lifting constant C_m . It is independent of the unknown solution w . Its dependence on T enters through powers of T and through a Mittag-Leffler factor of the form $E_\alpha(C_* T^\alpha)$.

Proof. Take $\psi = w(t)$ in (2.17). By Lemma 2.11 and the coercivity of B_t ,

$$\frac{1}{2} {}^C D_t^\alpha \|w(t)\|_{L^2}^2 + c_A \|w(t)\|_{H^m}^2 \leq \|G(t)\|_{(V_m^0)'} \|w(t)\|_{H^m}. \quad (3.2)$$

Using Young's inequality,

$$\frac{1}{2} {}^C D_t^\alpha \|w(t)\|_{L^2}^2 + \frac{c_A}{2} \|w(t)\|_{H^m}^2 \leq \frac{1}{2c_A} \|G(t)\|_{(V_m^0)'}^2. \quad (3.3)$$

The growth condition (2.12), Theorem 2.9, boundedness of B_t , and the lifting bounds give

$$\|G(t)\|_{(V_m^0)'}^2 \leq C \left(\|c_0(t)\|_{L^2}^2 + \|w(t)\|_{H^m}^2 + \|z(t)\|_{H^m}^2 + \|{}^C D_t^\alpha z(t)\|_{H^m}^2 \right). \quad (3.4)$$

Combining (3.3) and (3.4), absorbing the part that is controlled by coercivity when possible and treating the remaining lower-order contribution by Lemma 2.10, yields

$$\|w\|_{L^\infty(0,T;L^2)}^2 + \|w\|_{L^2(0,T;H^m)}^2 \leq C_T \left(\|w(0)\|_{L^2}^2 + \|c_0\|_{L^2(Q_T)}^2 + \|z\|_{H^1(0,T;H^m)}^2 \right). \quad (3.5)$$

Finally, from the equation,

$${}^C D_t^\alpha w = G - A(t)w,$$

and the boundedness of $A(t)$ from H^m to $(V_m^0)'$, we get the stated bound for ${}^C D_t^\alpha w$. The estimate (3.1) follows from Lemma 2.3. \square

Theorem 3.2 (Linear fractional solvability). *Under Assumption 2.4, for every $F \in L^2(0, T; (V_m^0)')$ and every $w_0 \in L^2(0, 1)$ compatible with V_m^0 in the usual weak sense, the linear problem*

$$\left\langle {}^C D_t^\alpha y(t), \psi \right\rangle + B_t(y(t), \psi) = \langle F(t), \psi \rangle, \quad y(0) = w_0, \quad (3.6)$$

has a unique weak solution $y \in L^2(0, T; V_m^0)$ with ${}^C D_t^\alpha y \in L^2(0, T; (V_m^0)')$, and

$$\|y\|_{L^2(0,T;V_m^0)} + \|{}^C D_t^\alpha y\|_{L^2(0,T;(V_m^0)')} \leq C_T \left(\|w_0\|_{L^2(0,1)} + \|F\|_{L^2(0,T;(V_m^0)')} \right). \quad (3.7)$$

Let \mathcal{S}_T denote the zero-initial solution operator $F \mapsto y$. We write

$$\delta(T, \alpha) := C_E \|\mathcal{S}_T\|_{L^2(0,T;(V_m^0)') \rightarrow L^2(0,T;V_m^0)}, \quad (3.8)$$

where C_E is the constant in $\|u\|_{L^2} + \|u_x\|_{L^2} \leq C_E \|u\|_{H^m}$ for $u \in V_m^0$. In the autonomous coercive case, the usual fractional resolvent estimate gives the representative bound

$$\delta(T, \alpha) \leq C_E C_{\alpha,A} \frac{T^\alpha}{\Gamma(1 + \alpha)}. \quad (3.9)$$

Proof. One may use a Galerkin basis of V_m^0 . The finite-dimensional fractional system is solved componentwise by the standard Volterra formulation. Testing the Galerkin equation by the approximate solution, using Lemma 2.11, (2.8), (2.9), and then applying weak compactness gives a limit satisfying (3.6). The same energy inequality applied to the difference of two solutions gives uniqueness. Estimate (3.7) follows exactly as in Theorem 3.1 with G replaced by F . The operator norm in (3.8) is therefore finite; estimate (3.9) is the standard consequence of the convolution representation by the fractional resolvent kernel in the autonomous case. \square

Theorem 3.3 (Existence of weak solution). *Assume 2.4–2.7. If*

$$L_g \delta(T, \alpha) < 1, \quad (3.10)$$

with $\delta(T, \alpha)$ defined in (3.8), then problem (1.1)–(1.4) admits a weak solution on $[0, T]$. In particular, for fixed L_g , the condition is satisfied on sufficiently short time intervals whenever the resolvent estimate (3.9) is available.

Proof. For $u \in L^2(0, T; V_m^0)$ define $\mathcal{T}u = w$, where w solves the linear problem

$${}^C D_t^\alpha w + A(t)w = g(x, t, u + z, (u + z)_x) - {}^C D_t^\alpha z - A(t)z, \quad w(0) = \phi - z(\cdot, 0). \quad (3.11)$$

The right-hand side belongs to $L^2(0, T; (V_m^0)')$ by Theorem 2.9 and Lemma 2.3, so Theorem 3.2 makes \mathcal{T} well defined. For $u_1, u_2 \in L^2(0, T; V_m^0)$, the initial and lifted terms cancel, and (2.11) gives

$$\begin{aligned} \|\mathcal{T}u_1 - \mathcal{T}u_2\|_{L^2(0, T; V_m^0)} &\leq \|\mathcal{S}_T\| L_g C_E \|u_1 - u_2\|_{L^2(0, T; V_m^0)} \\ &= L_g \delta(T, \alpha) \|u_1 - u_2\|_{L^2(0, T; V_m^0)}. \end{aligned} \quad (3.12)$$

Thus \mathcal{T} is a contraction under (3.10). Banach's fixed-point theorem yields a fixed point w , and $v = w + z$ is a weak solution of the original nonlocal problem. \square

Theorem 3.4 (Uniqueness and continuous dependence). *Under the assumptions of Theorem 3.3, the weak solution is unique. More precisely, if v_1 and v_2 correspond to data $(\phi_1, e_{0,1}, e_{2m-1,1})$ and $(\phi_2, e_{0,2}, e_{2m-1,2})$, then*

$$\begin{aligned} \|v_1 - v_2\|_{L^2(0, T; H^m(0,1))} &\leq C_T \left(\|\phi_1 - \phi_2\|_{L^2(0,1)} + \|e_{0,1} - e_{0,2}\|_{H^1(0, T)} \right. \\ &\quad \left. + \|e_{2m-1,1} - e_{2m-1,2}\|_{H^1(0, T)} \right), \end{aligned} \quad (3.13)$$

where C_T is independent of the two individual solutions.

Proof. Let z_i be the lift of $(e_{0,i}, e_{2m-1,i})$, let $y = w_1 - w_2$, and set $\zeta = z_1 - z_2$. The data-dependent forcing created by the lifts satisfies

$$\begin{aligned} \|\mathcal{F}_{\text{data}}\|_{L^2(0, T; (V_m^0)')} &\leq \left(\frac{T^{1-\alpha}}{\Gamma(2-\alpha)} + C_A + L_g C_E \right) C_m \\ &\quad \times \left(\|e_{0,1} - e_{0,2}\|_{H^1(0, T)} + \|e_{2m-1,1} - e_{2m-1,2}\|_{H^1(0, T)} \right). \end{aligned} \quad (3.14)$$

This inequality follows from (2.6), (2.7), boundedness of B_t , and the Lipschitz estimate for the part of g containing ζ .

Subtracting the two weak formulations and testing by y gives, after Lemma 2.11 and Young's inequality,

$${}^C D_t^\alpha \|y(t)\|_{L^2}^2 + c_A \|y(t)\|_{H^m}^2 \leq C_1 \|y(t)\|_{L^2}^2 + C \|\mathcal{F}_{\text{data}}(t)\|_{(V_m^0)'}^2, \quad (3.15)$$

where one may take, after adjusting embedding constants,

$$C_1 = 2C_E^2 \left(L_g + \frac{L_g^2}{c_A} \right). \quad (3.16)$$

Equivalently,

$$Y(t) \leq C_0 + \frac{\tilde{C}_1}{\Gamma(\alpha)} \int_0^t (t-s)^{\alpha-1} Y(s) ds, \quad Y(t) = \|y(t)\|_{L^2}^2, \quad \tilde{C}_1 = C_1 \Gamma(\alpha), \quad (3.17)$$

with C_0 controlled by $\|\phi_1 - \phi_2\|_{L^2}^2$ and (3.14). Lemma 2.10 yields

$$Y(t) \leq C_0 E_\alpha(\tilde{C}_1 t^\alpha),$$

and integrating (3.15) in time gives (3.13). If the data are identical, then $C_0 = 0$, so $v_1 = v_2$. \square

Corollary 3.5 (Finite-time continuation). *Suppose the hypotheses of Theorems 3.3 and 3.4 hold on each subinterval of $[0, T]$ and that the a priori bound in Theorem 3.1 remains finite on bounded time intervals. Then, the local weak solution can be continued step by step to the whole interval $[0, T]$.*

Proof. The fractional Gronwall factor is a Mittag-Leffler term $E_\alpha(Ct^\alpha)$, which is finite for every finite t . The continuation argument does not assert a uniform-in-time bound as $T \rightarrow \infty$; the constant may grow, and for large t the Mittag-Leffler function has exponential-type growth. What is needed for continuation on a prescribed finite interval is only that the norm controlling the next local step stays finite. This follows from Theorem 3.1 on bounded intervals and from the fact that the local existence time depends only on the structural constants and on the finite size of the data at the beginning of the step. \square

4. Representative numerical schemes

The analysis above is formulated for general m under Assumption 2.4. The computations below are more modest: they are designed to verify the nonlocal discretization mechanism for $m = 1$. This limitation is intentional and is stated explicitly. To make the numerical section closer to the analytical model, it contains not only the classical linear benchmark but also a variable-coefficient nonlinear manufactured example.

For $m = 1$, the model reduces to a second-order problem with two integral constraints. We first consider

$${}^C D_t^\alpha v(x, t) - v_{xx}(x, t) = f(x, t), \quad (x, t) \in (0, 1) \times (0, T), \quad (4.1)$$

with

$$v(x, 0) = \phi(x), \quad (4.2)$$

and

$$\int_0^1 v(\xi, t) d\xi = e_0(t), \quad \int_0^1 \xi v(\xi, t) d\xi = e_1(t). \quad (4.3)$$

4.1. L1 finite-difference discretization

Let $x_j = jh$, $j = 0, \dots, N$, with $h = 1/N$, and $t_n = n\tau$, $n = 0, \dots, M$, with $\tau = T/M$. The L1 approximation of the Caputo derivative is

$${}^C D_t^\alpha v(x_j, t_n) \approx \frac{1}{\Gamma(2 - \alpha)\tau^\alpha} \sum_{k=0}^{n-1} a_k (V_j^{n-k} - V_j^{n-k-1}), \quad a_k = (k + 1)^{1-\alpha} - k^{1-\alpha}. \quad (4.4)$$

Because $0 < 1 - \alpha < 1$, the function $s^{1-\alpha}$ is increasing and concave. Hence,

$$a_0 > a_1 > a_2 > \dots > 0, \quad (4.5)$$

and the normalization factor $\Gamma(2 - \alpha)\tau^\alpha$ is the standard L1 normalization for $0 < \alpha < 1$.

For the interior points $j = 1, \dots, N - 1$, we write

$$\frac{1}{\Gamma(2 - \alpha)\tau^\alpha} \sum_{k=0}^{n-1} a_k (V_j^{n-k} - V_j^{n-k-1}) - \frac{V_{j-1}^n - 2V_j^n + V_{j+1}^n}{h^2} = f(x_j, t_n). \quad (4.6)$$

No ghost points are required. The stencil at $j = 1$ uses V_0^n, V_1^n, V_2^n , and the stencil at $j = N - 1$ uses $V_{N-2}^n, V_{N-1}^n, V_N^n$. The two endpoint values V_0^n and V_N^n are unknowns and are determined simultaneously with the interior values by the two discrete integral constraints

$$h \sum_{j=0}^N \omega_j V_j^n = e_0(t_n), \quad (4.7)$$

$$h \sum_{j=0}^N \omega_j x_j V_j^n = e_1(t_n), \quad (4.8)$$

where $\omega_0 = \omega_N = 1/2$ and $\omega_j = 1$ for $1 \leq j \leq N - 1$. Therefore, each time level produces a square linear system for $V^n = (V_0^n, \dots, V_N^n)^T$.

For smooth solutions, the central difference in (4.6) is $O(h^2)$ and the trapezoidal approximations in (4.7) and (4.8) are also $O(h^2)$. Hence the spatial and quadrature contributions are consistent with each other. The standard L1 time error is $O(\tau^{2-\alpha})$ for sufficiently smooth solutions; therefore the expected total consistency scale is

$$O(\tau^{2-\alpha} + h^2). \quad (4.9)$$

When the time step is linked to the space step, the observed rate reflects the larger of these two contributions.

4.2. Picard discretization for a variable-coefficient nonlinear test

To address the nonlinear and variable-coefficient features of the model within the $m = 1$ computational setting, we also consider

$${}^c D_t^\alpha v - \partial_x((1+x)v_x) = \lambda \sin(v) + \mu v_x + q(x, t), \quad (4.10)$$

with the same two integral constraints. At time level t_n , the flux term is approximated by

$$\partial_x((1+x)v_x)(x_j, t_n) \approx \frac{a_{j+1/2}(V_{j+1}^n - V_j^n) - a_{j-1/2}(V_j^n - V_{j-1}^n)}{h^2}, \quad a_{j+1/2} = 1 + \frac{x_j + x_{j+1}}{2}. \quad (4.11)$$

The nonlinearity is treated by Picard iteration: for a current iterate $V^{n,(r)}$, the terms $\sin(V_j^n)$ and $(V_{j+1}^n - V_{j-1}^n)/(2h)$ on the right-hand side are evaluated at $V^{n,(r)}$, and the resulting linear system is solved for $V^{n,(r+1)}$. The two moment Eqs (4.7) and (4.8) are imposed at every Picard iterate.

5. Numerical simulations, examples, and tables

5.1. Example 1: manufactured-solution verification

Example 5.1 (Exact benchmark). Choose

$$v_{\text{ex}}(x, t) = (1 + t^2)(1 + x + x^2). \quad (5.1)$$

Then

$$\phi(x) = 1 + x + x^2, \quad (5.2)$$

$$e_0(t) = \int_0^1 v_{\text{ex}}(\xi, t) d\xi = \frac{11}{6}(1 + t^2), \quad (5.3)$$

$$e_1(t) = \int_0^1 \xi v_{\text{ex}}(\xi, t) d\xi = \frac{13}{12}(1 + t^2), \quad (5.4)$$

and the forcing term is

$$f(x, t) = \frac{\Gamma(3)}{\Gamma(3 - \alpha)} t^{2-\alpha} (1 + x + x^2) - 2(1 + t^2). \quad (5.5)$$

The second term in (5.5) is correct because $-v_{\text{ex},xx} = -2(1 + t^2)$.

For the main verification plots we use $\alpha = 0.6$, $T = 1$, $N = 60$, and $M = 240$. The numerical surface and the final-time comparison with the exact solution are shown in Figures 1 and 2.

Table 1 reports the maximum grid error and the RMS error for three mesh levels, while Figure 3 displays the corresponding log–log convergence curve. Together, the table and figure show a nearly second-order trend with respect to h for the chosen mesh sequence. This is consistent with the second-order central difference in space and the $O(h^2)$ trapezoidal enforcement of the integral constraints.

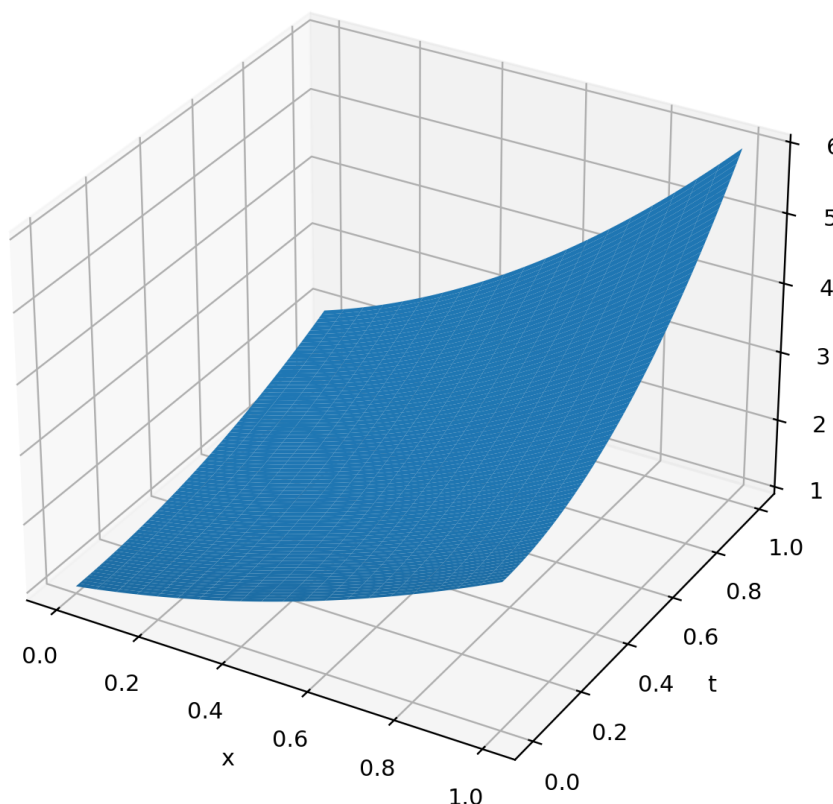


Figure 1. Numerical solution for the manufactured benchmark with $\alpha = 0.6$.

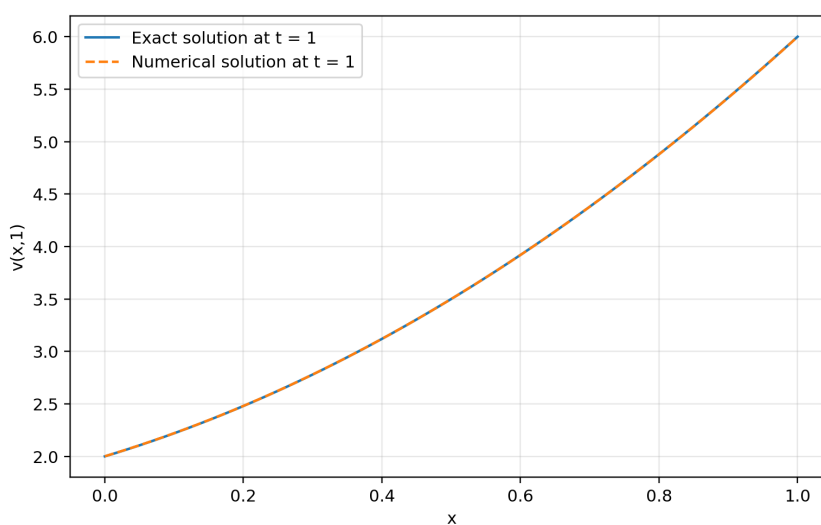


Figure 2. Comparison between the exact and numerical solutions at the final time $t = 1$ for the manufactured benchmark.

Table 1. Observed errors for the manufactured benchmark with $\alpha = 0.6$, where the maximum norm is taken over the discrete grid points (x_j, t_n) .

N	M	$\ v - v_h\ _{\infty, \text{grid}}$	RMS error	Observed rate
20	80	1.1217×10^{-2}	4.1665×10^{-3}	—
40	160	2.8403×10^{-3}	1.0214×10^{-3}	1.9816
80	320	7.2048×10^{-4}	2.5264×10^{-4}	1.9790

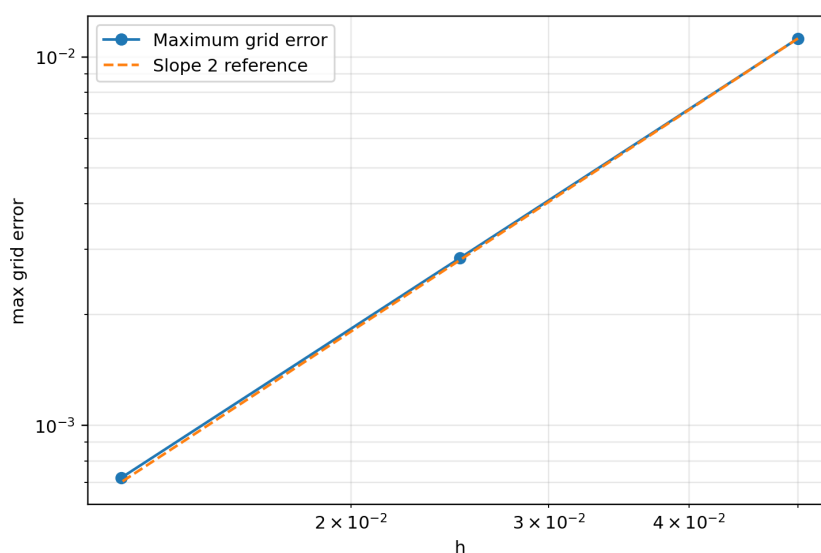


Figure 3. Observed convergence of the benchmark solver. The error profile is consistent with a second-order spatial trend for the selected mesh sequence.

5.2. Example 2: influence of the fractional order with compatible forcing

Example 5.2 (Parameter study in α). We solve

$${}^c D_t^\alpha v - v_{xx} = 10(6x^2 - 6x + 1)e^{-t}, \quad (5.6)$$

with zero initial data and homogeneous integral constraints,

$$\int_0^1 v(\xi, t) d\xi = 0, \quad \int_0^1 \xi v(\xi, t) d\xi = 0. \quad (5.7)$$

The spatial factor $6x^2 - 6x + 1$ satisfies

$$\int_0^1 (6x^2 - 6x + 1)dx = 0, \quad \int_0^1 x(6x^2 - 6x + 1)dx = 0. \quad (5.8)$$

The compatibility condition (1.4) is also satisfied because $\phi = 0$ and $e_0 = e_1 = 0$ at $t = 0$. The final-time profiles are computed for $\alpha \in \{0.3, 0.6, 0.9\}$.

Figure 4 compares the final-time profiles obtained for $\alpha = 0.3, 0.6$, and 0.9 , and Table 2 gives the corresponding maximum and L^2 amplitudes. The second experiment shows that, under the same compatible forcing and integral constraints, the response amplitude at the final time varies with the fractional order. Larger values of α produce a response closer to the classical parabolic behavior, while smaller values retain stronger memory effects.

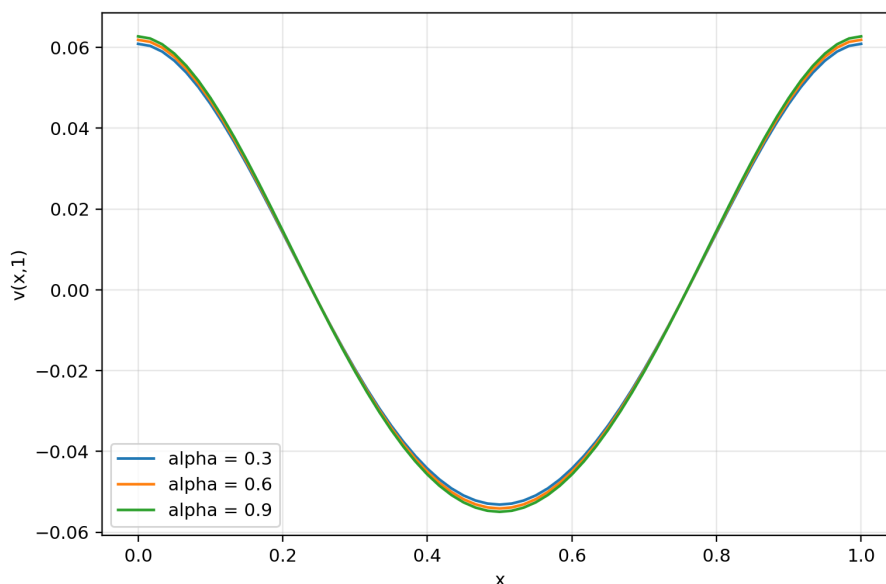


Figure 4. Effect of the fractional order on the profile $v(x, 1)$ under a common zero-moment forcing.

Table 2. Summary indicators for the parameter study at the final time $t = 1$.

α	$\max_{x \in [0,1]} v_h(x, 1) $	$\ v_h(\cdot, 1)\ _{L^2(0,1)}$
0.3	0.06087	0.03981
0.6	0.06186	0.04050
0.9	0.06271	0.04109

5.3. Example 3: variable-coefficient nonlinear manufactured test

Example 5.3 (Nonlinear test with exact solution). Consider (4.10) with

$$\lambda = 0.20, \quad \mu = 0.10, \quad v_{\text{ex}}(x, t) = (1 + t^2)(1 + x + x^2), \quad (5.9)$$

and with the same moment data (5.3) and (5.4). The manufactured term is

$$q(x, t) = \frac{\Gamma(3)}{\Gamma(3 - \alpha)} t^{2-\alpha} (1 + x + x^2) - (1 + t^2)(3 + 4x) - \lambda \sin((1 + t^2)(1 + x + x^2)) - \mu(1 + t^2)(1 + 2x). \quad (5.10)$$

Then v_{ex} solves (4.10). The nonlinear part $\lambda \sin(v) + \mu v_x$ is globally Lipschitz in (v, v_x) with Lipschitz constant not exceeding $|\lambda| + |\mu|$.

Figure 5 shows that the Picard solution agrees with the manufactured exact profile at $t = 1$. Table 3 quantifies this agreement by reporting the maximum grid error, the RMS error, the observed convergence rate, and the average number of Picard iterations. This third test is still restricted to $m = 1$, but it includes a variable coefficient and a nonlinear, gradient-dependent right-hand side. It therefore gives a numerical check closer to the analytical assumptions than the purely linear benchmark. The fully higher-order nonlinear discretization for $m > 1$ remains a separate numerical-analysis problem.

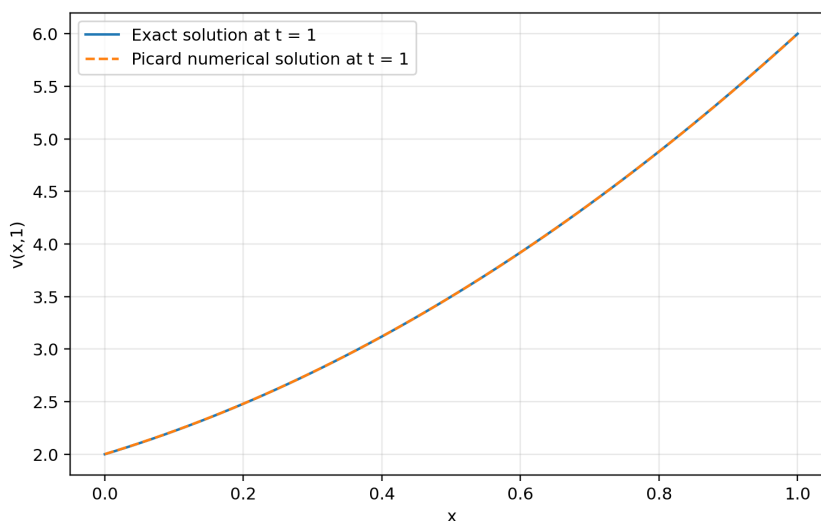


Figure 5. Final-time comparison for the variable-coefficient nonlinear manufactured test with $\alpha = 0.6$.

Table 3. Observed errors for the variable-coefficient nonlinear manufactured test with $\alpha = 0.6$, where the maximum norm is taken over the discrete grid.

N	M	$\ v - v_h\ _{\infty, \text{grid}}$	RMS error	observed rate	average Picard iterations
20	80	1.0552×10^{-2}	4.1781×10^{-3}	–	5.25
40	160	2.6348×10^{-3}	1.0232×10^{-3}	2.0018	4.99
80	320	6.5340×10^{-4}	2.5273×10^{-4}	2.0117	4.98

6. Discussion

The analytical part of the paper separates two issues that should not be conflated. The first is the treatment of the fractional derivative and the nonlocal moment constraints. This part is handled explicitly by the Caputo estimates, the lifting construction, and the weak formulation on V_m^0 . The second is the realization of the higher-order variable-coefficient operator. For nonconstant a , the derivatives of a produce lower-order terms, and the coercivity of the full weak form must be verified for the coefficient class under consideration or accepted as a structural assumption. This dependence is made explicit in the formulation.

The a priori estimate is the key stability statement. It shows that the solution norm is controlled by the initial datum, the forcing level in the nonlinear term, and the two integral boundary data. The constant may depend on the final time through a Mittag-Leffler factor, but it does not hide any dependence on the unknown solution. The existence theorem then uses the linear fractional problem as a proved auxiliary step rather than as an unexplained assumption, and the contraction constant is identified through the norm of the zero-initial solution operator.

The numerical results should be interpreted within their stated scope. Example 1 verifies the L1 finite-difference scheme and the direct enforcement of the two integral constraints. Example 2 uses a forcing with zero imposed moments, which removes an avoidable compatibility concern. Example 3 adds a variable coefficient and a nonlinear gradient-dependent term, thereby bringing the computation closer to the analytical model. The computations support the proposed nonlocal discretization for second-order problems. They do not constitute a complete numerical theory for arbitrary m .

7. Conclusions

We studied a time-fractional evolution equation with a variable-coefficient spatial operator, a nonlinear term depending on v and v_x , and purely integral boundary conditions. The paper provides a weak formulation based on a moment lifting, records the role of the coefficient derivatives in the operator order and coercivity, proves a priori stability and well-posedness under explicit structural assumptions, and gives reproducible computations for representative second-order cases.

For arbitrary m and variable coefficient a , the coercive weak realization must be verified in concrete settings. The numerical section is restricted to $m = 1$ and includes both linear and nonlinear variable-coefficient tests; the fully higher-order nonlinear numerical method is left for future work.

Several directions follow naturally. First, one should prove coercivity for specific classes of higher-order variable-coefficient operators under checkable boundary and coefficient conditions. Second,

the numerical analysis should be extended from $m = 1$ to $m > 1$, including nonlinear solvers and stability/error estimates for the resulting high-order nonlocal systems. Third, graded time meshes and adaptive strategies should be investigated to handle the weak initial singularities typical of fractional evolution equations. Extensions to multidimensional domains, inverse source problems, control, and data-driven parameter estimation with nonlocal constraints are also natural next steps.

Author contributions

Ahcene Merad: Contributed to the problem formulation, mathematical analysis, numerical implementation, and manuscript preparation; Abdellah Menasri: Contributed to the supervision of the analytical development, validation of the results, and final review of the manuscript. All authors read and approved the final manuscript.

Use of Generative-AI tools declaration

The authors declare that they have not used Artificial Intelligence (AI) tools in the creation of this article.

Acknowledgments

The authors sincerely thank the Editor of AIMS Mathematics and the anonymous reviewers for their valuable comments and constructive suggestions, which significantly helped improve the quality and clarity of this manuscript.

Conflict of interest

Prof. Ahcene Merad is the Guest Editor of special issue “Advances in Differential Equations: Methods and Applications” for AIMS Mathematics. Prof. Ahcene Merad was not involved in the editorial review and the decision to publish this article.

The authors declare no conflicts of interest.

References

1. I. Podlubny, *Fractional differential equations: an introduction to fractional derivatives, fractional differential equations, to methods of their solution and some of their applications*, San Diego, CA: Academic Press, 1999. [https://doi.org/10.1016/S0076-5392\(99\)x8001-5](https://doi.org/10.1016/S0076-5392(99)x8001-5)
2. A. A. Kilbas, H. M. Srivastava, J. J. Trujillo, *Theory and applications of fractional differential equations*, Amsterdam: Elsevier, 2006.
3. S. G. Samko, A. A. Kilbas, O. I. Marichev, *Fractional integrals and derivatives: theory and applications*, Yverdon: Gordon and Breach Science Publishers, 1993.
4. K. Diethelm, *The analysis of fractional differential equations: an application-oriented exposition using differential operators of Caputo type*, Berlin: Springer, 2010. <https://doi.org/10.1007/978-3-642-14574-2>

5. Y. Lin, C. Xu, Finite difference/spectral approximations for the time-fractional diffusion equation, *J. Comput. Phys.*, **225** (2007), 1533–1552. <https://doi.org/10.1016/j.jcp.2007.02.001>
6. B. Jin, R. D. Lazarov, Z. Zhou, An analysis of the L1 scheme for the subdiffusion equation with nonsmooth data, *IMA J. Numer. Anal.*, **36** (2016), 197–221. <https://doi.org/10.1093/imanum/dru063>
7. K. Sakamoto, M. Yamamoto, Initial value/boundary value problems for fractional diffusion-wave equations and applications to some inverse problems, *J. Math. Anal. Appl.*, **382** (2011), 426–447. <https://doi.org/10.1016/j.jmaa.2011.04.058>
8. A. Ashyralyev, E. Ozturk, On a difference scheme of second order of accuracy for the Bitsadze-Samarskii type nonlocal boundary-value problem, *Bound. Value Probl.*, **2014** (2014), 14. <https://doi.org/10.1186/1687-2770-2014-14>
9. R. Yan, S. Sun, Y. Sun, Z. Han, Boundary value problems for fractional differential equations with nonlocal boundary conditions, *Adv. Differ. Equ.*, **2013** (2013), 176. <https://doi.org/10.1186/1687-1847-2013-176>
10. C. Derbazi, H. Hammouche, Caputo-Hadamard fractional differential equations with nonlocal fractional integro-differential boundary conditions via topological degree theory, *AIMS Math.*, **5** (2020), 2694–2709. <https://doi.org/10.3934/math.2020174>
11. N. H. Tuan, N. A. Triet, N. H. Luc, N. D. Phuong, On a time fractional diffusion with nonlocal in time conditions, *Adv. Contin. Discret. Model.*, **2021** (2021), 204. <https://doi.org/10.1186/s13662-021-03365-1>
12. C. Nuchpong, S. K. Ntouyas, D. Vivek, J. Tariboon, Nonlocal boundary value problems for ψ -Hilfer fractional-order Langevin equations, *Bound. Value Probl.*, **2021** (2021), 34. <https://doi.org/10.1186/s13661-021-01511-y>
13. Z. Li, X. Huang, Y. Liu, Initial-boundary value problems for coupled systems of time-fractional diffusion equations, *Fract. Calc. Appl. Anal.*, **26** (2023), 533–566. <https://doi.org/10.1007/s13540-023-00149-0>
14. J. Hou, X. Meng, J. Wang, Y. Han, Y. Yu, Local error estimate of an L1-finite difference scheme for the multiterm two-dimensional time-fractional reaction–diffusion equation with Robin boundary conditions, *Fractal Fract.*, **7** (2023), 453. <https://doi.org/10.3390/fractalfract7060453>
15. R. Luca, A. Tudorache, On a system of Hadamard fractional differential equations with nonlocal boundary conditions on an infinite interval, *Fractal Fract.*, **7** (2023), 458. <https://doi.org/10.3390/fractalfract7060458>
16. A. Tudorache, R. Luca, Systems of Hilfer–Hadamard fractional differential equations with nonlocal coupled boundary conditions, *Fractal Fract.*, **7** (2023), 816. <https://doi.org/10.3390/fractalfract7110816>
17. S. Sitho, S. K. Ntouyas, C. Sudprasert, J. Tariboon, Systems of sequential ψ_1 -Hilfer and ψ_2 -Caputo fractional differential equations with fractional integro-differential nonlocal boundary conditions, *Symmetry*, **15** (2023), 680. <https://doi.org/10.3390/sym15030680>
18. J. Zhao, S. Dong, Z. Fang, A mixed finite element method for the multi-term time-fractional reaction–diffusion equations, *Fractal Fract.*, **8** (2024), 51. <https://doi.org/10.3390/fractalfract8010051>

19. P. Priyanka, S. Arora, S. Sahani, S. Singh, Numerical study of multi-term time-fractional sub-diffusion equation using hybrid L1 scheme with quintic Hermite splines, *Math. Comput. Appl.*, **29** (2024), 100. <https://doi.org/10.3390/mca29060100>
20. E. Alhazzani, S. Mesloub, H. E. Gadain, On the solvability of a singular time fractional parabolic equation with non classical boundary conditions, *Fractal Fract.*, **8** (2024), 189. <https://doi.org/10.3390/fractalfract8040189>
21. M. Alghanmi, S. Alqurayqiri, Existence results for a coupled system of nonlinear fractional functional differential equations with infinite delay and nonlocal integral boundary conditions, *AIMS Math.*, **9** (2024), 15040–15059. <https://doi.org/10.3934/math.2024729>
22. N. Alghamdi, B. Ahmad, E. A. Alharbi, W. Shammakh, Investigation of multi-term delay fractional differential equations with integro-multipoint boundary conditions, *AIMS Math.*, **9** (2024), 12964–12981. <https://doi.org/10.3934/math.2024632>
23. S. F. Aljurbua, Extended existence results for FDEs with nonlocal conditions, *AIMS Math.*, **9** (2024), 9049–9058. <https://doi.org/10.3934/math.2024440>
24. J. Liu, K. Zhang, X. Xie, The existence of solutions of Hadamard fractional differential equations with integral and discrete boundary conditions on infinite interval, *Electron. Res. Arch.*, **32** (2024), 2286–2309. <https://doi.org/10.3934/era.2024104>
25. W. M. Abd-Elhameed, Y. H. Youssri, A. G. Atta, Adopted spectral tau approach for the time-fractional diffusion equation via seventh-kind Chebyshev polynomials, *Bound. Value Probl.*, **2024** (2024), 102. <https://doi.org/10.1186/s13661-024-01907-6>
26. L. Brugnano, K. Burrage, P. Burrage, F. Iavernaro, A spectrally accurate step-by-step method for the numerical solution of fractional differential equations, *J. Sci. Comput.*, **99** (2024), 48. <https://doi.org/10.1007/s10915-024-02517-1>
27. D. Kim, K. Woo, Sobolev spaces and trace theorems for time-fractional evolution equations, *Potential Anal.*, **63** (2025), 1289–1333. <https://doi.org/10.1007/s11118-025-10205-4>
28. A. Salem, R. Al-Maalwi, Fractional evolution equation with nonlocal multi-point condition: application to fractional Ginzburg–Landau equation, *Axioms*, **14** (2025), 205. <https://doi.org/10.3390/axioms14030205>
29. K. Aldwoah, A. Ali, B. A. I. Younis, M. Almalahi, A. Touati, Analysis of hybrid fractional differential equations with nonlocal boundary conditions and linear perturbations, *Bound. Value Probl.*, **2025** (2025), 47. <https://doi.org/10.1186/s13661-025-02038-2>
30. H. A. Hamarashid, M. F. Hama, P. O. Sabir, S. M. El-Deeb, A. Catas, Solutions of nonlinear integro-differential equations of fractional order defined using fractional boundary conditions, *J. Inequal. Appl.*, **2025** (2025), 88. <https://doi.org/10.1186/s13660-024-03235-w>



AIMS Press

©2026 the Author(s), licensee AIMS Press. This is an open access article distributed under the terms of the Creative Commons Attribution License (<https://creativecommons.org/licenses/by/4.0>)